2024 IEEE International Conference on Robotics and Automation (ICRA)
May 13-17, 2024. Yokohama, Japan

Leveraging Tethers for Distributed Formation Control of Simple Robots

Sadie Cutler[1] and Kirstin Petersen[2]

2024 IEEE International Conference on Robotics and Automation (ICRA) | 979-8-3503-8457-4/24/$31.00 ©2024 IEEE | DOI: 10.1109/ICRA57147.2024.10611041

***Abstract*— Tethers have great potential in multi-robot systems from enabling retrieval of deployed robots and facilitating power transfer, to use by the robots as a net or partition. In this paper, we show in simulation that tethers can also be used to do distributed formation control on very simple robots. Specifically, our simulated agents are connected in series by un-actuated, flexible, fixed-length tethers and use tether angle and strain, in conjunction with the physical constraints of the tethers, to adjust their position with respect to their neighbors. This presents a significant simplification over traditional formation control which, at a minimum, requires exteroceptive sensors to perceive bearing and/or distance to nearby agents. We present and evaluate an algorithm on a large set of transitions between formations with 5 agents and an example transition with 35 agents. The convergence time grows with the number of agents, however, the memory and computation time per agent remain constant. Future work will investigate the ability to use tethers and strain for reactive behaviors and more diverse tasks.**

I. Introduction

Tethers, taut and loose, have been used in robotics to provide power and stabilization [1], ensure recoverability [2], [3], assist with object capture [4], [5], to aid construction [6], [7] and more. In this paper, we show that tethers can also be used to enable individual agents in a collective to navigate relative to the location of their connected neighbors using proprioceptive sensing, leading to distributed formation control. This is in spite of the lack of planning and explicit communication, and the fact that individual agents react only to present information and do not know or sense the current or desired state of any other agent in the collective.

Formation control is a classic challenge for multi-robot systems with example applications spanning the ability to maintain communication networks while navigating hostile or dynamic environments; encapsulate and transport objects; and present moving displays for entertainment purposes [8]. Past formation studies have relied on everything from planners [9] and centralized controllers [10] with global knowledge and sensing, to local communication radii [11], and limited sensing [12]. Such robot collectives may accomplish more than individual robots, but coordination can be a challenge, especially in situations where the hardware or the surroundings pose restrictions on sensing and communication, e.g. in GPS-denied environments like space or in low-visibility and bandwidth-restricted environments like the deep sea.

This work was funded by a Packard Fellowship for Science and Engineering and NSF #2042411.

[2]School of Electrical and Computer Engineering, Cornell University, Ithaca, NY 14853, USA kirstin@cornell.edu

[1]Sibley School of Mechanical and Aerospace Engineering, Cornell University, Ithaca, NY 14853, USA sc3236@cornell.edu

In this paper, we explore the extreme case - where an arbitrary number of mobile agents connected in series by fixed-length, passive, un-actuated tethers coordinate to produce goal formations in 2D solely by keeping their two affixed tethers taut and observing their local strain and angle and monitoring for close-range collision avoidance. We present a simple algorithm that combines the objectives of keeping the tethers taut and making progress towards the desired relative bearing between the agent and its neighbors. In this paper, we purposefully work with agents that are not fixed to a point in space and have no global attraction to gain a better understanding of system dynamics. While the convergence time on particular formations increases with the size of the collective, the memory and computation required by individual agents remain the same. Beyond the applications described above, this strategy can serve as a backup in case more sophisticated communication or sensing fails in systems that already require a tether, e.g. robots connected by nets for oil spill clean-up, or for types of robots that typically lack exteroceptive sensors, such as soft robots.

The contribution of this paper straddles several sub-fields in robotics. In Sec. II, we first discuss how tethers are currently used with robots, then elaborate briefly on different means of formation control. Next, we define the scope of our research and the related simulation framework alongside particular evaluation metrics and tested transitions (Secs. III-IV). Our approach, outlined in Sec. V and Fig. 1, combines objective vectors based on the desired relative angle

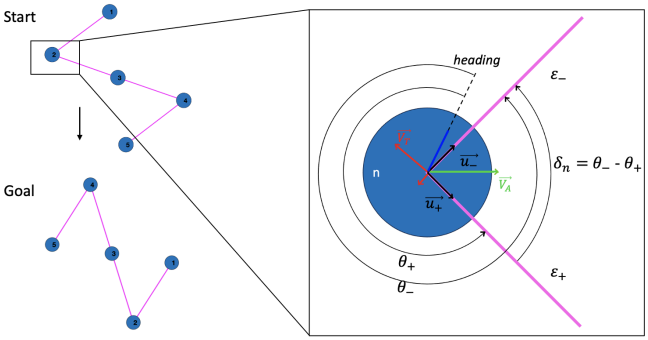

Fig. 1: Example of a tethered collective and its start and goal formation. The blow-out shows the information available to the n-th agent, including current angle (θ) and strain (ε) in the previous ($-$) and next ($+$) tethers, measured in the reference frame of the agent. Unit vectors, u, indicate the direction of strain, $\overrightarrow{V_A}$ shows the force resulting from the desired relative angle, and $\overrightarrow{V_T}$ shows the force resulting from the desire to keep the tether taut.

between tethers and nominal tether strain into a resultant velocity. We describe the results of these tests in Sec. VI and discuss conclusions and avenues for future work in Sec. VII. Our work paves the way for broader applications of tethered multi-agent systems for use where vision or sensing/communication capabilities are limited, making simple, robust solutions imperative.

II. Related Work

Previous work with tethered robots falls into two categories: 1) the tether is performing a function that is primary to the task and robots facilitate the task by moving the tether, e.g. nets, partitions; or 2) the robots are performing a task and the tethers facilitate their operation, thus performing a secondary function such as additional power or stability. In ground robots, taut secondary tethers are used for recovery of single and multiple robots and for localization and mapping of individuals [2], [13]. The principal use of secondary tethers has been as a source of power or data transfer for quadcopters [14]. Tethers have also been used with quadcopters to extend the sensing range (either with fixed- [15] or sliding-tether connections [1]) and taut tethers have been used for flight and landing stability [3] and the length and angle of tethers have been used as control inputs [16].

Despite additional time and energy expended, constraining a tether to be taut makes it possible to use the force on the tether and its relative angle to estimate and control the position of a robot, foregoing the need for external sensing. This has been demonstrated in simulation and with limited hardware implementation for single quadcopters in both fixed- [17] and variable-length tethers [12].

On the topic of formation control, the method is generally defined by available sensors and means of communication [8]. Designs trade-off sensing and communication; with absolute or long-range sensors agents can forego communication, with inter-agent communication they may rely on more localized sensors [18]. The latter involves distributed control strategies [19]: In bearing-based formation control, agents measure the bearings of neighboring agents using vision or sensor-arrays, often without the need for communication [20]. Distance-based formation control works similarly, but estimates or measures the distance between agents. Our method, most similar to [21], uses a combination of distance- and bearing-based control on each agent to achieve distributed formation control. Unlike their work, however, our agents are connected physically, work asynchronously, do not require a leader, are trying to fulfill both distance constraints and angle goals in each time step, employ minimal (interoceptive) sensing, and use distance-and bearing-based algorithms to generate vectors, which combined, form a cohesive control strategy.

III. System Model

To demonstrate our algorithm, we implemented a simulation framework in MATLAB. We simulate N circular agents operating on a plane, connected in series by fixed-length tethers. We assume that the tether connections are frictionless and rotate separately from the agent's heading. The agents have holonomic motion and do not communicate. To approximate asynchronous operation, we update agents in random order in each time step. To perform collision avoidance, each agent can sense nearby objects i.e. nearby agents since our environment is obstacle-free (we do not currently assume that they can sense unattached tethers).

The agents can distinguish between their two tethers and, when tethers are taut, can sense their tethers' relative angle, $\delta_n = \theta_+ - \theta_-$ and strains $\varepsilon_{+,-}$ (Fig. 1). A key aspect of the tether's use for control and sensing is tautness; below the minimum strain, we assume the tether is slack and the agent loses its ability to accurately measure the relative angle of its neighbor. For ease, tethers are always represented as a straight line in the simulation, with a quantity identifying the state of the tether (loose, taut, or stretched).

To achieve distributed formation control, we provide a goal formation for the collective at the beginning of the simulation in the form of a set of desired differences between tether angles, $\delta_{n,goal}$. Each agent is only aware of its own goal.

All agents are free to move and we do not consider incentives created by external sensors, nor the desire for a global pose of the collective. By eliminating this layer of control, we can study the dynamics of the formation changes directly.

In this paper, we focus on 5-agent simulations but also show an example with 35 agents. Each agent has a diameter, $D = 5$, and we scale our objectives such that their maximum step size and speed per time step equals $D/2$. We set the un-stretched tether length, $L_u = 5D$ and choose a Young's modulus of $E = \ 60MPa$, similar to Paracord Type I. We consider the admissible limits of tether slack or elongation to be ± 2.5, corresponding to 10% of the tether length; well within the 30% elongation that the Paracord can sustain. Although we are currently developing specialized hardware, as an example which contextualizes forces of taut tethers, these values would support operation with the popular Jackal UGV from Clearpath Robotics which can pull 20-40lbs depending on the terrain – on the scale of the force required for tether elongation, but does not exceed the Paracord's breaking force of 95 lbs.

IV. Evaluation Metrics

Formations are defined as a list of differences between tether angles, δ, for all agents with two tethers. We define a successful transition between formations if the current angle difference, δ, is within $\pm 5^\circ$ of δ_{goal} for all agents with two tethers. We classify transitions as failed if 1) agents cannot converge to their goal within 6,000 time steps, 2) tethers collide, or 3) if tether strain falls outside of the 0-10% range. We are interested in the fraction of successful transitions, the convergence time, t_c, and the cumulative distance, d_c (which would be related to the energy expenditure). For comparison, we also compute optimal cumulative distance, d_o, computed by overlaying the start and goal configuration median and summing up the pairwise distances between agents

To evaluate the algorithm, we generated all possible permutations of formations with 5 agents given a resolution of 15° between adjoining tethers, and eliminated all with tether/agent collisions. Only agents with two tethers compute angle differences and can have corresponding goals assigned; i.e. each formation consists of $\{\delta_{2,goal}, \delta_{3,goal}, \delta_{4,goal}\}$. We used this set as start formations, and matched them with goals consisting of the same set of formations randomly shuffled for a total of 1,830 transitions. We further hand-crafted six transitions to evaluate the ability of the system to handle differing numbers and placements of active agents in unconverged states (Fig. 2):

- **A:** $\{\pi/2; -\pi/2; \pi/2\} \rightarrow \{-\pi/2; \pi/2; -\pi/2\}$
  Neighboring agents have opposite goals, they work together and there are no competing constraints.
- **B:** $\{\pi; \pi/3; \pi\} \rightarrow \{\pi; -\pi/3; \pi\}$
  A change is only imposed on the center agent (agent 3).
- **C:** $\{\pi/4; \pi; -\pi/4\} \rightarrow \{-\pi/4; -\pi; \pi/4\}$
  A change is imposed on both agents 2 and 3.
- **D:** $\{\pi; \pi; \pi/2\} \rightarrow \{\pi; \pi; -\pi/2\}$
  Similar to B only one agent has an imposed change, but this agent is located off-center (agent 4).
- **E:** $\{\pi/4; \pi; \pi/4\} \rightarrow \{3/4\pi; \pi; 3/4\pi\}$
  Agents on either side of the center agent try to increase their respective δ_n by moving towards the center of the formation.
- **F:** $\{\pi; \pi; \pi\} \rightarrow \{3/5\pi; 3/5\pi; 3/5\pi\}$
  All agents attempt to decrease δ_n simultaneously, by moving away from the center of the formation.

Transitions E and F are especially interesting in that they both produce directly conflicting actions between agents, as will be described further in the results.

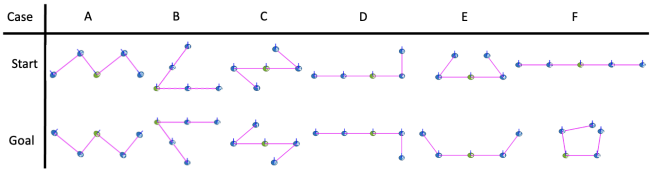

Fig. 2: Start and goal formations for hand-crafted transitions.

V. Algorithm

To achieve distributed formation control, the agents compute three vectors to update their position. These are related to their perceived tether angles and strain, and close-range collision avoidance. This strategy is similar in concept to the original Boids model [22], but relies on proprioceptive sensing of tethers, rather than exteroceptive sensing. It is worth noting that because the implementation of our algorithm separates rotation and translation of each robot, it can support both holonomic and non-holonomic motion.

A. Objective 1: Angle Difference

We designed objective 1 to encourage agents to drive in the direction that decreases the error between current- and desired- difference in tether angles. This vector is a function of the error:

$$\overrightarrow{V_A} = sign(\delta_{goal} - \delta)\sqrt{\frac{|\delta_{goal} - \delta|}{2\pi}}\frac{\overrightarrow{u}_- + \overrightarrow{u}_+}{|\overrightarrow{u}_- + \overrightarrow{u}_+|} \quad (1)$$

Where $\overrightarrow{u}_-$ and $\overrightarrow{u}_+$ are unit vectors pointing toward the tethered neighbors and $sign$ returns +1, 0, or -1 depending on the sign of the error signal. The idea is that agents can increase the tether angle difference by driving toward the tether mean and decrease it by driving in the opposite direction. Effectively, this objective causes the agent to move further per time step when the error is large and is a simple way to alter the angle with minimal sensory input. Note again that agents at the end of the configuration have only one tether and are not influenced by this objective.

B. Objective 2: Tether Tautness

Because the agents rely on the tether for localization with respect to their neighbors, they must aim to keep it taut at all times. To do this, we impose the following vector for each tether on each agent:

$$\overrightarrow{V_T} = sign(\varepsilon - \varepsilon_u)(\varepsilon - \varepsilon_u)^2\overrightarrow{u} \quad (2)$$

where ε and $\overrightarrow{u}$ correspond to either ε_+ and $\overrightarrow{u}_+$ or ε_- and $\overrightarrow{u}_-$ depending on whether the computation is for the tether leading to the previous or next agent in the collective. The idea is that there is a region of optimal strain where the tether is taut enough to give accurate angle readings but not unduly pulling on adjacent agents.

C. Objective 3: Collision Avoidance

To prevent physical overlap between agents, we assume they have access to a close-range sensor, e.g. IR sensors, located on their perimeter. We compute this repulsive force for agents whose centers are located closer than $2.5D$ to the center of the agent in question. This way, we prevent collisions even when agents are moving at their maximum speed. The magnitude is computed as:

$$\overrightarrow{V_{Ob}} = 8De^{-\frac{d^2}{2(D/2)^2}}\overrightarrow{u}_{Ob} \quad (3)$$

i.e. a Gaussian with $\sigma = D/2$ and amplitude = 8D, where d is the distance from the center of the agent to the sensed obstacle(s). The unit vector $\overrightarrow{u}_{Ob}$ points from the center of the obstacle to the center of the agent.

D. Resultant Vector

The resultant vector which gives the orientation and magnitude of the agent velocity is computed as the scaled sum of the three vectors described above:

$$\overrightarrow{V} = c_A\overrightarrow{V_A} + c_T(\overrightarrow{V}_{T_-} + \overrightarrow{V}_{T_+}) + \overrightarrow{V}_{Ob} \quad (4)$$

To find the appropriate values of scalars c_A and c_T, we performed a parameter sweep (Fig. 3) on 150 randomly chosen transitions out of the full set of 1,830 discussed earlier. We see that the fraction of successful runs is fairly robust to variations in c_A and c_T, and that there is a sweet spot in which this fraction remains high, but failures due to

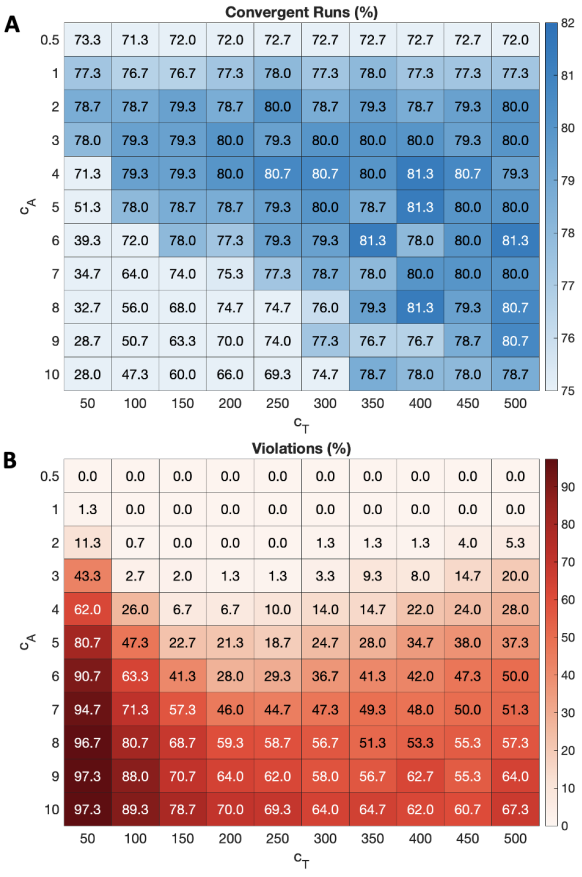

Fig. 3: Parameter sweep of angle and tether scalars, c_A and c_T, evaluated for 150 random transitions. A) shows the percentage of transitions that successfully converge; B) shows the percentage of transitions that fail due to tether strain violations.

tether-strain violations are less likely. Based on the sweep, we chose to continue with the combination $c_A = 2$ and $c_T = 250$. A proportion test on all possible parameter pairs assessing convergence produced a p-value of 4.79e-152, allowing us to reject the null hypothesis and ascertain that there is a significant difference in the probability of success between parameter pairs. Pairwise comparisons of convergence between the chosen parameter pair and all remaining parameter pairs without violations, revealed that there was not a statistically significant difference in the outcome between any of these pairs, indicating, that although the parameter pairs have significant impact on convergence, there is some leeway in parameters chosen. With our chosen parameters, we see 81% successful runs and no violations of the tether strain. 5% of the runs failed due to tether collisions, and the remaining 14% of the runs failed due to a stagnation behavior in which all agents were moving, but none of the relative tether angles were changing over time. We expand upon this phenomenon in Sec. VI.

VI. Results & Discussion

We ran the complete algorithm on the full set of 1,830 transitions as well as the 6 hand-crafted transitions discussed in Sec. IV. We found that 73.5% of the cases successfully converged to the goal; 7.3% failed due to tether collisions; and 19.1% failed to converge as discussed below. No violations of tether strain were observed.

A. Converged runs

Fig. 5 shows the sequence by which the 5-agent collective reached the goal in the handcrafted transitions A-D. Interestingly, an emergent outcome of the algorithm is that the collective unfolds forming a near-straight line before converging, when the transitions are such that from start to goal all δ either remain at π or change between $< \pi$ and $\geq \pi$. This may seem trivial because to maintain taut tethers individual angles need to pass through $\delta = pi$, but the fact that all agents in the collective reach this point nearly simultaneously is less intuitive. Although we stop the simulation when convergence criteria were met (Sec.IV), if allowed to run well past convergence, we see little to no translation of any of the agents.

The convergence time was $\{t_{c,A} = 90, t_{c,B} = 275, t_{c,C} = 321, t_{c,D} = 126\}$ time steps. In other words, the time seems to be affected by both the overall change in angle differences and the number of neighbors that interact positively. However, we also found that transitions where only one agent has an incentive to change its angle difference cause considerable drift, d_d, $\{d_{d,A} = 8.5, d_{d,B} = 129.1, d_{d,C} = 3.0, t_{d,D} = 44.29\}$. Fig. 4 shows t_c and d_c, of all successfully completed transitions. Predictably, we see that higher t_c generally require agents to travel further. We also see that transitions with similar t_c can result in different d_c and that this discrepancy grows as t_c increases.

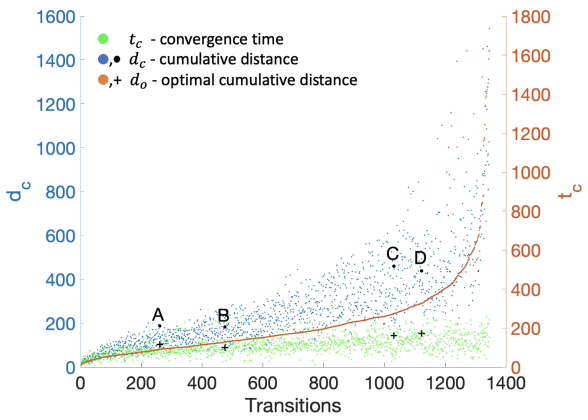

Fig. 4: Transition performance analysis.

In Fig. 4, we see that agents who are coordinating only through tether strain have to move significantly further than in the optimal case and we notice the same in the compilation videos - without a fixed agent or global attraction, the collective often drifts significantly while correcting their angle differences.

B. Failures due to collisions

Collisions can occur in our system because we do not assume that agents have the ability to perceive unattached tethers, which we anticipate would be hard to incorporate

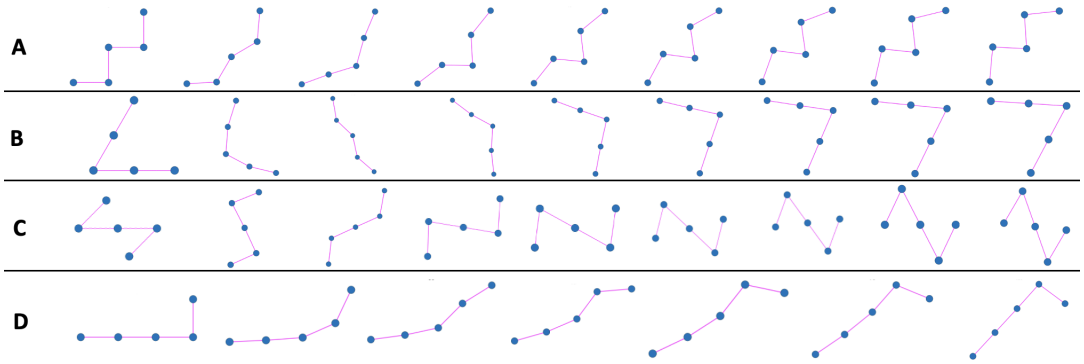

Fig. 5: Snapshots of transitions of hand-crafted cases A, B, C, and D from Fig. 2. The key time steps exhibited are as follows: A:0,10,20,30,40,50,60,70,85; B:0,35,70,105,140,175,210,245,280; C:0,40,80,120,160,200,240,280,325; D:0,15,30,45,75,90,125.

reliably in hardware. Transition E in Fig. 2 is an example of when a collision occurs. Driven by objective 1, agents 2 and 4 attempt to move towards the center of the collective to increase their angle differences. Agent 3 starts at its goal angle, and works to keep it there. This means that forces on the tether generated by agent 2 translate to agent 4 and vice versa, causing objective 2 to dominate over 1, creating a resultant vector that points away from the center of the collective. Agents 1 and 5 each have only one tether and therefore ignore objective 1. Because they have no information about what their respective neighbors are trying to achieve, they drift inwards causing the whole collective to eventually collapse with crossed tethers. While such scenarios only happen in 7.3% of our 1,830 5-agent simulations, we expect increasing risk with larger collectives and more complex formations. A cursory investigation indicated that this phenomenon only occurs when $\delta_{n,goal} < \pi/2$ for both agents 2 and 4.

C. Failures due to stagnation

The most common failure scenario involved stagnation where agents started moving with a joint heading (circular or linear motion), but were unable to make any progress toward the desired formation. Transition F is an example of this case (Fig. 6). Here, agents 2, 3, and 4 all compute resultant vectors that point away from the center of the collective in an attempt to decrease their angle differences. At first, progress is made, however, once any two non-adjacent tethers, i.e. tethers leading from agents 1 to 2 and 4 to 5, become parallel (and not co-linear) the resultant vectors of all agents align and the collective drifts rather than producing formation change. Again, agents 1 and 5 exacerbate the problem because they have no incentive other than avoiding collisions and keeping their tether taut. We found that this undesired stable state was characteristic of all stagnation failures, and that it never occurred in successful runs. We also found that it was so stable that even the incorporation of a significant stochastic back-off mechanism to help agents break ties, would only perturb the collective temporarily.

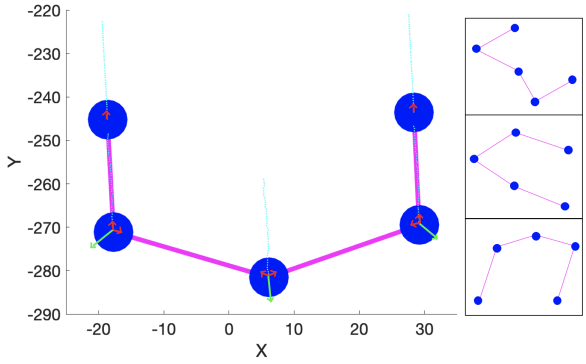

Fig. 6: Left: Stagnation during transition F, over 85 time steps (trail shown with dots). Arrows indicate objective vectors as in Fig. 1. Right: Other examples of stagnant formations.

D. Predicting the Outcome of Transitions

By looking at a few key features of each formation transition and using a decision tree, we were able to predict the outcome of the 1,830 tested transitions for a 5-agent collective with 91.1% accuracy (Fig. 7). Specifically, our decision tree correctly predicted 96.9% of all converged transitions, 88.0% of all stagnated cases, and 45.8% of all collisions. The two features we used for branching in the decision tree were: 1) if the leading and trailing tethers were both pointed inward in the start or goal formation, and 2) how aligned all of the $\overrightarrow{V_A}$ were in the starting formation (quantified by taking their standard deviation). To quantify whether the leading and trailing tethers were both pointed inward, we projected an extension of the leading and trailing tethers onto the start and goal formations and, if those projection lines intersected, measured the distance from the center agent to the intersection point.

Stepping through the decision tree: beginning at 1, if there is an intersection in the goal formation (2B), the case is unlikely to converge and predictions on whether it is likely to stall or collide are based on existence of an intersection (2B) and intersection distance (3C) in the start formation. If there is no intersection in the goal formation (2A) or the start formation (3A), then the case is predicted to either converge or stall based on magnitude of the standard

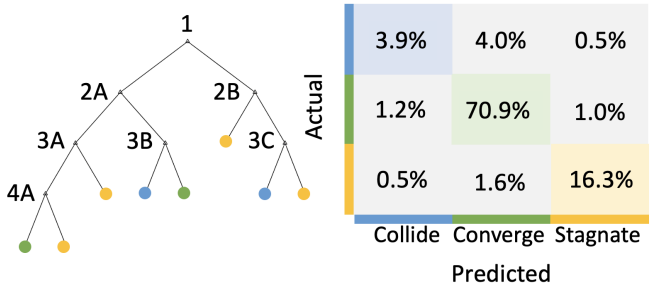

Fig. 7: The decision tree (left) and accompanying confusion matrix (right) where a colored square indicates an accurate prediction.

deviation of resultant vectors in y (3A) and x (4A). If there is no intersection in the goal formation (2A) but there is in the start formation (3B), then the case is predicted to either converge or collide based on the start formation's intersection distance.

E. Scaling up the collective

A key advantage of the algorithm is that the memory and computational constraints of the individual agents are independent of the size of the collective. To investigate t_c, and cumulative distance normalized by optimal cumulative distance, d_c/d_o, we scaled up two versions of case A: 1) repeats the original pattern and 2) scales up the shape (Fig. 8). Generally, t_c and d_c/d_o grows with the size of the collective, but in the second case larger collectives must cover much greater cumulative distance which explains why t_c grows faster than in the first case.

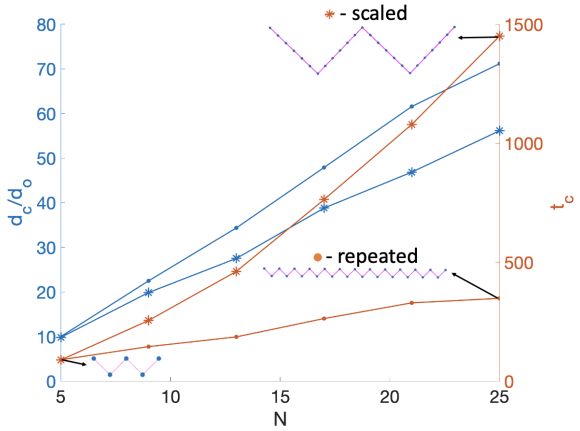

Fig. 8: As indicated by the inserts on the right, we assessed increasing collective sizes for the repeated pattern and the scaled shape.

Finally, the demo shown in Fig. 9 demonstrates a 35-agent collective transitioning from an egg-like shape to a bird in flight. It is worth reiterating here that this occurs in spite of the fact that agents have access to their own state in terms of strain and angle of their affixed tethers and their goal.

VII. Conclusion

In this paper, we investigated the ability of a collective of tethered, mobile agents to perform formation control

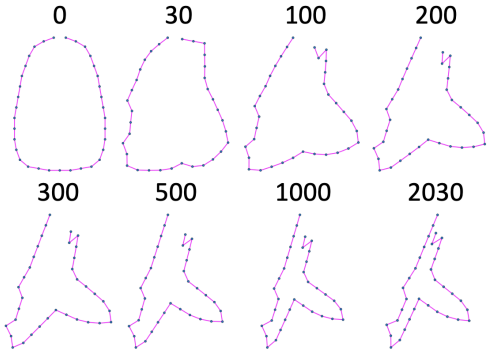

Fig. 9: 35 agents transitioning from an outline of an egg to a bird in flight.

by relying only on the strain and angle of their affixed tethers and close-range collision sensors. Specifically, we investigated through simulation the ability of 5 such agents to switch between pairs of 1,830 randomly-generated formations. Our algorithm successfully enabled 1,345 or 73.5% transitions to converge. We found that the failures fell into two categories: 1) collisions due to the lack of tether sensing and 2) stagnation in which the collective is moving, but no progress is made towards the goal; a decision tree can help us predict and avoid these problematic transitions. We increased collective size, demonstrating that while algorithm memory and computation time per agent remain constant, the t_c increases with the number of agents due to greater d_c. Finally, we presented a demonstration with 35 agents transitioning between the outline of an egg to a bird in flight. While there is more work to be done to improve the success rate of the algorithm, this is a promising result for collectives composed of simple robots, or for use as a back-up mechanism in case more sophisticated coordination mechanisms fail. Passive tethers can remain lightweight and inexpensive, yet help distributed agents stay connected, do containment and encapsulation tasks and, with the introduction of this work, formation control. Since each agents' algorithm accounts for only local effects and recomputes objectives at each time step, we expect that the collective can remain agile in changing environments and tasks.

We plan to improve our algorithm and find solutions to the two types of failed cases seen in this paper; both issues which may be addressed by predicting and avoiding related formations, mitigating their impact by adding intermediate goals, or adding additional dexterity to leading and trailing agents. In addition, we see many avenues for future work including exploration of: 1) algorithm resilience to agent heterogeneity, e.g in sensing, update intervals, speed; 2) addition of global attraction, such as way-point navigation or targets for encapsulation; and 3) enabling general obstacle avoidance. Constraining a tether to be taut reduces the risk of entanglement and limits the operation space which can be helpful for planning purposes, but may require additional energy expenditure and robustness to system disturbances. Studies of these potential downsides present another interesting avenue for future research. Finally, of course, we hope to translate these insights into real hardware.

REFERENCES

[1] B. Kosarnovsky and S. Arogeti, "Geometric and constrained control for a string of tethered drones," *Robotics and Autonomous Systems*, vol. 133, p. 103609, 2020. [Online]. Available: https://www.sciencedirect.com/science/article/pii/S0921889020304498

[2] H. Sato, K. Uchiyama, F. Ito, R. Sawahashi, and T. Nakamura, "Distributed deployment with multiple moving robots for long distance complex pipe inspection," *IEEE Robotics and Automation Letters*, vol. 7, no. 4, pp. 11 252–11 259, 2022.

[3] S.-R. Oh, K. Pathak, S. K. Agrawal, H. R. Pota, and M. Garratt, "Approaches for a tether-guided landing of an autonomous helicopter," *IEEE Transactions on Robotics*, vol. 22, no. 3, pp. 536–544, 2006.

[4] F. Zhang, P. Huang, Z. Meng, Y. Zhang, and Z. Liu, "Dynamics analysis and controller design for maneuverable tethered space net robot," *Journal of guidance, control, and dynamics*, vol. 40, no. 11, pp. 2828–2843, 2017.

[5] Y. Su, Y. Jiang, Y. Zhu, and H. Liu, "Object gathering with a tethered robot duo," *IEEE Robotics and Automation Letters*, vol. 7, no. 2, pp. 2132–2139, 2022.

[6] B. Felbrich, M. Prado, S. Saffarian, J. Solly, L. Vasey, J. Knippers, A. Menges, *et al.*, "Multi-machine fabrication: an integrative design process utilising an autonomous uav and industrial robots for the fabrication of long-span composite structures," 2017.

[7] K. Zhang, P. Chermprayong, F. Xiao, D. Tzoumanikas, B. Dams, S. Kay, B. B. Kocer, A. Burns, L. Orr, C. Choi, *et al.*, "Aerial additive manufacturing with multiple autonomous robots," *Nature*, vol. 609, no. 7928, pp. 709–717, 2022.

[8] Q. Chen, Y. Wang, Y. Jin, T. Wang, X. Nie, and T. Yan, "A survey of an intelligent multi-agent formation control," *Applied Sciences*, vol. 13, no. 10, p. 5934, 2023.

[9] Z. Pan, D. Wang, H. Deng, and K. Li, "A virtual spring method for the multi-robot path planning and formation control," *International Journal of Control, Automation and Systems*, vol. 17, pp. 1272–1282, 2019.

[10] R. Carelli, C. De la Cruz, and F. Roberti, "Centralized formation control of non-holonomic mobile robots," *Latin American applied research*, vol. 36, no. 2, pp. 63–69, 2006.

[11] J. Alonso-Mora, E. Montijano, T. Nägeli, O. Hilliges, M. Schwager, and D. Rus, "Distributed multi-robot formation control in dynamic environments," *Autonomous Robots*, vol. 43, no. 5, pp. 1079–1100, 2019.

[12] X. Xiao, Y. Fan, J. Dufek, and R. Murphy, "Indoor uav localization using a tether," in *2018 IEEE International Symposium on Safety, Security, and Rescue Robotics (SSRR)*. IEEE, 2018, pp. 1–6.

[13] P. McGarey, K. MacTavish, F. Pomerleau, and T. D. Barfoot, "Tslam: Tethered simultaneous localization and mapping for mobile robots," *The International Journal of Robotics Research*, vol. 36, no. 12, pp. 1363–1386, 2017.

[14] L. Fagiano, "Systems of tethered multicopters: modeling and control design," *IFAC-PapersOnLine*, vol. 50, no. 1, pp. 4610–4615, 2017.

[15] M. Bolognini and L. Fagiano, "Lidar-based navigation of tethered drone formations in an unknown environment," *IFAC-PapersOnLine*, vol. 53, no. 2, pp. 9426–9431, 2020.

[16] R. Naldi, A. Gasparri, and E. Garone, "Cooperative pose stabilization of an aerial vehicle through physical interaction with a team of ground robots," in *2012 IEEE International Conference on Control Applications*. IEEE, 2012, pp. 415–420.

[17] S. Lupashin and R. D'Andrea, "Stabilization of a flying vehicle on a taut tether using inertial sensing," in *2013 IEEE/RSJ International Conference on Intelligent Robots and Systems*. IEEE, 2013, pp. 2432–2438.

[18] K.-K. Oh, M.-C. Park, and H.-S. Ahn, "A survey of multi-agent formation control," *Automatica*, vol. 53, pp. 424–440, 2015.

[19] Y. Liu, J. Liu, Z. He, Z. Li, Q. Zhang, and Z. Ding, "A survey of multi-agent systems on distributed formation control," *Unmanned Systems*, pp. 1–14, 2023.

[20] M. H. Trinh, S. Zhao, Z. Sun, D. Zelazo, B. D. Anderson, and H.-S. Ahn, "Bearing-based formation control of a group of agents with leader-first follower structure," *IEEE Transactions on Automatic Control*, vol. 64, no. 2, pp. 598–613, 2018.

[21] S. A. Barogh and H. Werner, "Cascaded formation control using angle and distance between agents with orientation control (part 1)," in *2016 UKACC 11th International Conference on Control (CONTROL)*. IEEE, 2016, pp. 1–6.

[22] C. W. Reynolds, "Flocks, herds and schools: A distributed behavioral model," in *Proceedings of the 14th annual conference on Computer graphics and interactive techniques*, 1987, pp. 25–34.